sustainability

MDPI

Article

Multi-Model and Multi-Scenario Assessment of Macroalgal Blue Carbon Potential: A Case Study of Zhejiang, China

Tengteng Wang [1,2,*], Li Song [2], Yue Xu [2], Bo Lin [2], Xuexi Xiao [2], Saixia Ying [2] and Guang Gao [1,*]

[1] State Key Laboratory of Marine Environmental Science, College of Ocean and Earth Sciences, Xiamen University, Xiamen 361005, China
[2] Zhejiang Zhongyi Testing Research Institute Co., Ltd., Ningbo 315040, China; songli@zynb.com.cn (L.S.); xuyue@zynb.com.cn (Y.X.); linbo@zynb.com.cn (B.L.); xiaoxuexi@zynb.com.cn (X.X.); yingsaixia@zynb.com.cn (S.Y.)
* Correspondence: 22320181152098@stu.xmu.edu.cn (T.W.); guang.gao@xmu.edu.cn (G.G.); Tel.: +86-188-5002-4392 (T.W.)

Abstract

Macroalgae are an important yet underrepresented component of marine blue carbon systems, but regional-scale assessments integrating historical dynamics, environmental drivers, future scenarios, and economic implications remain limited. This study developed an integrated framework to evaluate the macroalgal blue carbon potential of Zhejiang Province, China, a major macroalgal mariculture region. Using multi-source datasets from 2001 to 2023, we analyzed production trends, identified the environmental and socioeconomic factors most strongly associated with production, and projected future production and carbon sequestration under three management scenarios using four predictive approaches. Results showed that macroalgal production increased from 2.83×10^4 tonnes in 2001 to 14.60×10^4 tonnes in 2023, with total mariculture production as the dominant associated socioeconomic factor. Average annual carbon sequestration during 2006–2023 was estimated at 4176 t C (15,327 t CO_2 equivalent), increasing rapidly after 2017. Under the baseline scenario, cumulative sequestration during 2023–2042 was projected at approximately 2.67×10^5 t C, while active expansion could raise sequestration potential by approximately 12%. Economic valuation indicated that carbon credits contribute only 0.45–0.76% of product value, insufficient alone to provide a strong economic incentive for large-scale implementation. This study demonstrates the potential of macroalgal mariculture as a nature-based blue carbon solution and provides a transferable framework for coastal carbon management and climate mitigation strategies.

Keywords: blue carbon; carbon sequestration; economic valuation; macroalgae; scenario analysis

Check for updates

Academic Editor: Pablo Peri

Received: 7 August 2026
Revised: 26 September 2026
Accepted: 26 September 2026
Published: 30 September 2026

Copyright: © 2026 by the authors. Licensee MDPI, Basel, Switzerland. This article is an open access article distributed under the terms and conditions of the Creative Commons Attribution (CC BY) license.

1. Introduction

The ocean, as Earth's largest active carbon reservoir, stores approximately 93% of Earth's actively cycling carbon and provides a substantial sink for anthropogenic CO_2, playing an irreplaceable role in regulating the global carbon cycle [1]. In this context, the concept of "blue carbon" has emerged, referring specifically to carbon capture and long-term sequestration through biomass accumulation and sediment burial in coastal and marine ecosystems [2–4]. Traditional blue carbon research has focused primarily on three ecosystem types: mangroves, seagrass beds, and salt marshes. These ecosystems possess

well-characterized carbon sequestration mechanisms, mature stock assessment methodologies, and have been incorporated into international carbon accounting frameworks [5]. However, recent scientific advances have highlighted the substantial and previously underestimated role of macroalgae in marine carbon sequestration [6].

Global macroalgal carbon sequestration is estimated at 0.17–1.0 Pg C yr^{-1}, a magnitude comparable to the combined total of mangroves and seagrass beds [6–8]. This substantial carbon sink potential has prompted increasing calls for the inclusion of macroalgae in national and international blue carbon inventories and carbon trading mechanisms [9–11]. China is the world's largest macroalgal mariculture producer, accounting for over 60% of global production in 2022 [12]. Chinese macroalgal aquaculture is characterized by high-density, intensive cultivation systems, primarily involving *Saccharina japonica*, *Neopyropia yezoensis*, and *Gracilariopsis lemaneiformis* [13]. These cultured macroalgae not only provide food, feed, and industrial raw materials but also deliver significant ecosystem services, including carbon sequestration, nutrient removal, and habitat provision [14–18].

At the national scale, studies have estimated that China's macroalgal mariculture sequesters millions of tonnes (t) of carbon annually [13,19,20]. The species composition in Zhejiang was dominated by *Porphyra* (51.83%), followed by *Laminaria* (27.73%), *Sargassum fusiforme* (12.72%), and *Enteromorpha prolifera* (1.27%). Recent studies indicate that Zhejiang's macroalgal mariculture area proportion increased from 5.45% (2003) to 20.96% (2021) of the national total, representing a nearly four-fold increase [21]. Zhejiang contributes 53–71% of the nation's Expandable Aquaculture Area and 33–46% of total carbon sink increment potential. These findings underscore Zhejiang's growing importance in national macroalgal carbon sequestration.

Despite growing recognition of macroalgal carbon sequestration, several critical knowledge gaps persist. First, there is a scarcity of province-scale assessments using updated data, as most existing studies have focused on national scales or relied on data from the 1990s–2010s, and updated assessments incorporating recent production trends (2015–2023) with refined carbon accounting parameters are urgently needed to support current policy-making and carbon trading project development [13,20–22]. Second, the environmental regulatory mechanisms remain unclear: although macroalgal production is governed by multiple factors including water temperature, nutrient availability, and terrigenous inputs, the relative contributions of these factors and their response characteristics at the provincial scale have yet to be sufficiently quantified, limiting predictive capacity [6,14,23–25]. Third, multi-scenario future projections remain insufficient, as traditional linear models struggle to capture threshold effects and interactions in environment–production relationships, while machine learning applications in marine carbon sink prediction are still nascent, particularly for multi-scenario projections under different management strategies [26,27]. Fourth, economic valuation at realistic carbon prices is limited, given that while theoretical carbon sequestration values are frequently calculated, assessments using actual market carbon prices (e.g., China's certified emission reduction auction prices) are scarce, thereby constraining policy relevance [28–30].

It is worth emphasizing that this study advances beyond previous regional and national assessments of macroalgal carbon sequestration. Existing assessments for China remain largely confined to national-scale, aggregate estimates based on static coefficients and trend extrapolation [13,19,20], and few provide species-disaggregated, province-level accounts or evaluate the predictive reliability of the underlying production models. This study addresses these limitations through four methodological advances rather than a mere dataset update. First, we assemble a species-resolved dataset (*Porphyra* spp., *Laminaria japonica*, *Gracilariopsis lemaneiformis*, *Sargassum fusiforme*, and *Enteromorpha prolifera*) covering 2006–2023, and derive a production-weighted carbon content (27.25% DW) that is

cross-validated against the published literature, replacing the single national coefficients used previously. Second, candidate statistical and machine-learning models of algal production (MLR, RFR, TSE, and EC-TS) are screened using stationarity and cointegration diagnostics followed by leave-one-out and rolling-origin cross-validation, so that model selection is based on out-of-sample predictive skill rather than in-sample fit. Third, scenario projections are constructed with socio-economic and environmental drivers following trajectories anchored at trend-fitted 2023 levels, with uncertainty propagated via Monte Carlo simulation (N = 500) and reported as multi-model ensemble medians and intervals, instead of unvalidated trend extrapolation. Finally, the resulting sequestration estimates are linked to economic valuation using an actual market transaction price with price sensitivity analysis. Together, these elements provide a reproducible provincial-scale framework that complements existing national and global assessments.

This study takes Zhejiang Province, China, as a typical subtropical coastal province case to construct a macroalgal carbon sequestration assessment framework applicable to provincial-scale blue carbon management, with four specific objectives: (1) to quantify the current macroalgal carbon sequestration capacity in Zhejiang Province using updated production data (2001–2023) and species-specific carbon content parameters from published literature; (2) to identify the key environmental and socioeconomic drivers of spatiotemporal variation in macroalgal production and quantify their relative importances using correlation analysis and multiple predictive models; (3) to project future macroalgal production and carbon sequestration potential under three management scenarios—Baseline Continuation, Expansion with Intervention, and Static Freeze—through 2042; and (4) to conduct economic valuation of carbon sequestration using the Xiangshan first-order blue carbon auction price (106 RMB/t CO_2) and analyze the sensitivity of economic returns to carbon price variations.

2. Materials and Methods

2.1. Study Area

Zhejiang Province is located on the southeastern coast of China, with geographic coordinates spanning 118°00′–123°10′ E and 27°06′–31°03′ N. The province covers a land area of approximately 101,800 km^2 and a sea area of approximately 260,000 km^2, with a total coastline length of 6486 km (including 1840 km mainland coastline and 4646 km island coastline). The study focuses on the coastal waters of Zhejiang, encompassing major mariculture zones including Xiangshan Harbor, Sanmen Bay, Yueqing Bay, and the Zhoushan Archipelago (Figure 1).

The study area features a subtropical monsoon climate, with annual mean temperatures of 16–18 °C (January: 4–6 °C; July: 28–30 °C) and sea surface temperatures varying annually from 8 to 29 °C, with winter sea surface temperatures elevated relative to comparable latitudes by the Taiwan Warm Current branch. Annual precipitation ranges from 1300 to 1900 mm, concentrated in the May–September typhoon season, which influences terrigenous nutrient inputs and coastal salinity regimes. Salinity shows pronounced seasonal variation, with nearshore winter salinity decreasing to 28–30 under the influence of the Yangtze diluted water, while summer offshore water intrusion raises salinity to 30–32. Hydrodynamically, Xiangshan Harbor is a semi-enclosed bay with water exchange cycles of approximately 30–60 days that favor nutrient accumulation.

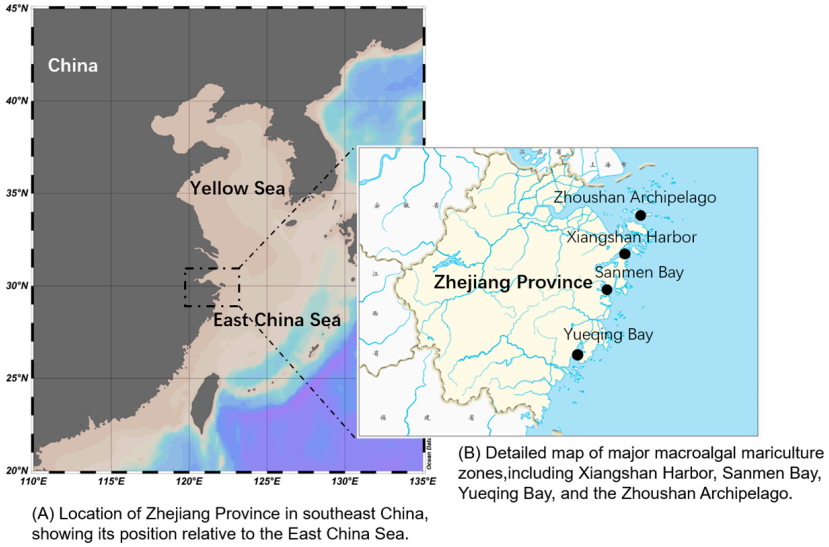


Figure 1. Study area map of Zhejiang Province, China.

2.2. Macroalgal Mariculture Systems and Species Composition

Macroalgal mariculture in Zhejiang has a long history, with Xiangshan Harbor, Sanmen Bay, and Zhoushan serving as the core production zones. The species composition is dominated by *Neopyropia* spp. (*Porphyra*; 51.83% of production), followed by *Saccharina japonica* (syn. *Laminaria japonica*; 27.73%), *Sargassum fusiforme* (12.72%), *Gracilariopsis lemaneiformis* (6.45%), and *Enteromorpha prolifera* (1.27%) (Figure 2) [20,31,32]. These five taxa also represent the major cultivated macroalgae of China's coastal provinces, whose national distribution is shown in Figure 3 [31,32].

The main cultured species include Saccharina japonica, a cold-temperate brown alga (*Phaeophyceae*) with optimal growth at 5–15 °C, cultured from November to May primarily in northern coastal waters at 5–15 m depth [31]; *Neopyropia yezoensis*, a warm-temperate red alga (*Rhodophyta*) with optimal growth at 10–20 °C, cultured from September to February using the shell-net plane culture method in southern coastal waters, with this species being dominant in Zhejiang by production volume due to its high carbon content and cultivation efficiency; *Gracilariopsis lemaneiformis*, a warm-water red alga (*Rhodophyta*) with optimal growth at 15–25 °C, culturable year-round and used primarily as agar raw material and abalone feed [33]; *Sargassum fusiforme*, a warm-temperate brown alga (*Phaeophyceae*) that is primarily wild-harvested with some cultivation in Dongtou waters [34]; and Enteromorpha prolifera, a eurythermal green alga (*Chlorophyta*) that is a wild species frequently forming seasonal green tide blooms in summer in mariculture zones [35,36] and, although not commercially cultivated, contributes to wild macroalgal biomass and carbon cycling. Species-specific carbon and water contents are summarized in Table 1. Other macroalgae cultivated elsewhere in China (e.g., *Undaria pinnatifida*, *Eucheuma* spp., and *Gelidium* spp.) fall outside Zhejiang's production accounting and are not considered further.

Table 1. Species-specific carbon content and water content parameters used in this study.

Species	Carbon Content (% Dry Weight)	Production Proportions in Zhejiang (%)	Water Content (%)	Source
Porphyra purpurea	27.35	51.83	80–85	[20,31]
Laminaria japonica	26.55	27.73	88–92	[20,31]
Gracilariopsis lemaneiformis	27.30	1.87 [a]	~85	[19,21]

Table 1. *Cont.*

Species	Carbon Content (% Dry Weight)	Production Proportions in Zhejiang (%)	Water Content (%)	Source
Sargassum fusiforme	28.39	12.72	~85	[20,31]
Enteromorpha prolifera	26.62	1.27	~85	[19,21]
Weighted Average	27.25	--	~85	Calculated

Note: The weighted average of 27.25% reported in Table 1 can be exactly reproduced as (27.35 × 0.5183 + 26.55 × 0.2773 + 27.30 × 0.0187 + 28.39 × 0.1272 + 26.62 × 0.0127) ÷ 0.9542 = 27.25%. The weighted average (27.25% DW) was calculated from the species-specific carbon contents [20,31] weighted by the production proportions reported in ref. [20]. An independent recalculation using alternative literature values [20,21] yields 27.96% DW, a difference of <3%, confirming that the results are robust to the choice of carbon-content parameters. [a] From 2014 Zhejiang production data (800 t of 42,724 t total) reported by Lü et al. (2018) [37]; the other four portions are 1999–2012 averages from ref. [20].

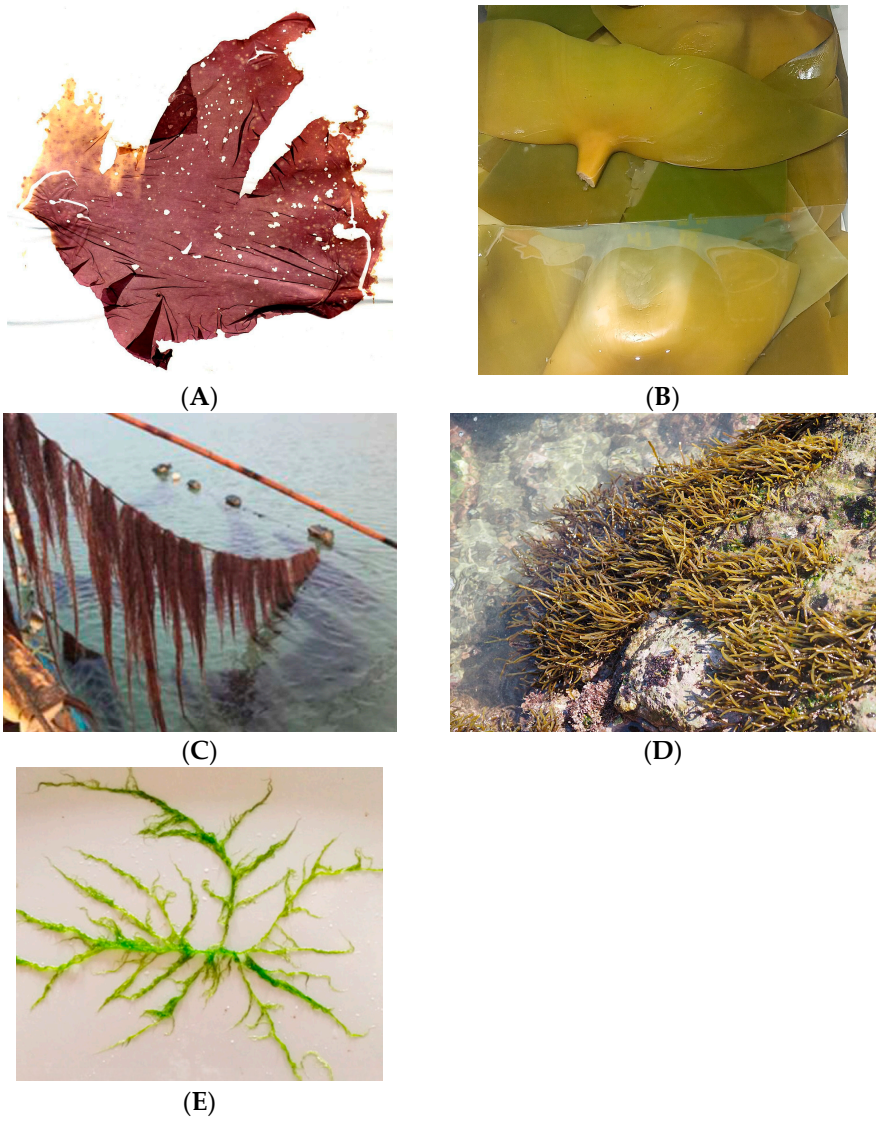


Figure 2. The major cultivated macroalgal species and culture systems in Zhejiang. (**A**) *Porphyra purpurea* (Image credit: Gabriele Kothe-Heinrich, via Wikimedia Commons, CC-BY-SA-3.0). (**B**) *Laminaria japonica* (Image credit: Fumikas Sagisavas, via Wikimedia Commons, CC0 1.0). (**C**) *Gracilariopsis lemaneiformis* (Image credit: [38], Figure 1e, CC BY 4.0). (**D**) *Sargassum fusiforme* (Image credit: merec0, via Wikimedia Commons, CC-BY-2.0). (**E**) *Enteromorpha prolifera* (Image credit: [39], Figure 1B, CC BY 4.0).

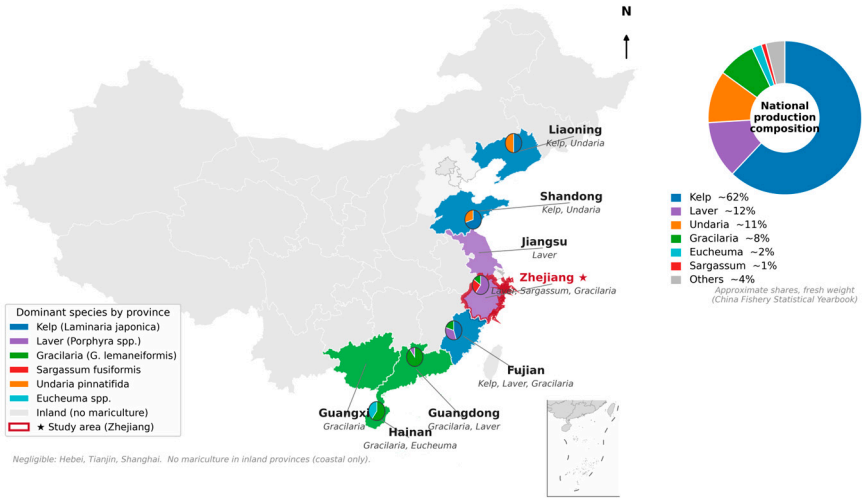


Figure 3. The national distribution of macroalgal mariculture in China. The map shows provincial macroalgal production (2023, China Fishery Statistical Yearbook [32]), the dominant cultivated taxa by region, and the location of the study area (Zhejiang, starred).

According to the Zhejiang Statistical Yearbook, macroalgal mariculture production in Zhejiang exhibited an overall increasing trend during 2001–2023, rising from 2.83 $\times$ 10^4 t (2001) to 14.60 $\times$ 10^4 t (2023). Although ecological conservation policies led to the retirement of some nearshore mariculture zones, resulting in area reduction from 109.06 $\times$ 10^3 ha (2006) to 84.26 $\times$ 10^3 ha (2023), technological advances and species optimization continuously improved per-unit-area yields, maintaining stable total production growth. Notably, production accelerated dramatically after 2017, increasing from 5.34 $\times$ 10^4 t (2016) to 14.60 $\times$$10^4$ t (2023), a 2.7-fold increase in just seven years.

2.3. Coastal Ecological Environment and Anthropogenic Influences

The ecological environment of Zhejiang's coastal waters is influenced by both natural processes and anthropogenic activities. Natural processes include the southward transport of nutrients by the Yangtze River diluted water, which provides material foundations for macroalgal growth; the semi-enclosed morphology of Xiangshan Harbor and Sanmen Bay, which promotes nutrient retention and extended water residence times, supporting high macroalgal productivity; and the convergence front formed by the Taiwan Warm Current and coastal currents, which creates productive upwelling zones. Anthropogenic activities stem from Zhejiang's role as an important industrial and economic province in eastern China, with major industrial facilities distributed along the coast, while urban domestic sewage and agricultural non-point source pollution enter the ocean through rivers, increasing nitrogen and phosphorus loads, and intensive mariculture activities (fish, shellfish, macroalgae) simultaneously modify local hydrodynamic conditions and nutrient cycling patterns. According to the Zhejiang Province Marine Environment Bulletin [40], key water quality parameters in mariculture zones include inorganic nitrogen (exceeding standards in some seasons), active phosphate (occasionally exceeding standards), and chemical oxygen demand (generally meeting standards); Xiangshan Harbor and Sanmen Bay are identified as key mariculture zones with relatively high nutrient levels suitable for macroalgal growth.

This complex environmental background—combining natural nutrient enrichment from riverine inputs, semi-enclosed bay hydrodynamics, intensive anthropogenic nutrient loading, and high-density mariculture activities—provides a representative scenario for studying macroalgal carbon sink environmental response mechanisms in subtropical coastal waters.

2.4. Data Collection and Sources

This study integrates multi-source data spanning 2001–2023, including annual macroalgal production (10^4 t) and mariculture area (10^4 ha) from the Zhejiang Statistical Yearbook and China Fishery Statistical Yearbook; total mariculture production (10^4 t) from the Zhejiang Statistical Yearbook; industrial water consumption (10^8 m^3) and domestic water consumption (10^8 m^3) from the Zhejiang Statistical Yearbook; and annual rainfall (mm) and annual mean temperature (°C) from the Zhejiang Statistical Yearbook and meteorological records. Because the period 2001–2005 has partial missing values for some variables while 2006–2023 has complete data for all variables, all analyses using multiple variables are restricted to 2006–2023 (n = 18 years). Species-specific carbon content and water content parameters were derived from the published literature (Table 1), and the weighted average carbon content was calculated based on species composition ratios for Zhejiang Province. In addition, to test whether the association between macroalgal production and total mariculture production is affected by part–whole correlation (macroalgal production being a component of the total), an alternative predictor, Culture_ex, was constructed as total mariculture production excluding macroalgal production.

2.5. Predictive Models

Four models were employed to project macroalgal production from 2023 to 2042: (1) Multiple Linear Regression (MLR), a transparent baseline relating macroalgal production to its strongest socioeconomic correlates; following multicollinearity diagnostics (variance inflation factors) and parsimony criteria (AIC/BIC), a two-predictor specification was adopted, with total mariculture production (coefficient 0.123, $p < 0.001$) and industrial water use (-0.142, $p = 0.092$; Newey–West HAC standard errors) as predictors ($R^2 = 0.980$ on historical data); (2) Random Forest Regression (RFR) [26], a non-linear ensemble model that captures complex interactions and threshold effects between environmental variables and macroalgal production, configured with 200 estimators, max_depth = 5 and min_samples_split = 5 to limit overfitting on the small sample, but without extrapolation capability—when future environmental conditions exceed the historical training range, predictions converge to the mean response at the training boundary, and RFR is therefore interpreted as a conservative lower bound; (3) Time Series Extrapolation (TSE), Holt's linear-trend exponential smoothing [41], relying solely on historical temporal patterns without incorporating external environmental variables; and (4) Environmentally Constrained Time Series (EC-TS), which combines trend extrapolation with environmental adjustment: historical growth rates are modulated by environmental suitability scores (temperature, mariculture scale, industrial water, domestic water) via sigmoid transformations. In EC-TS, the sigmoid centers are data-derived (historical means: mariculture 105.3×10^4 t, industrial water 25.6×10^8 m^3, domestic water 14.5×10^8 m^3), and the temperature response follows a Gaussian suitability function centered at 20 °C, consistent with the physiological optima of the dominant cultivated species (Section 2.2); by contrast, the sigmoid slopes and component weights are heuristic, expert-assigned parameters; EC-TS is therefore used as a scenario exploration tool rather than a statistically estimated model. No model is designated as primary a priori; model adequacy is assessed out-of-sample (Section 3.3), and headline projections are reported as the ensemble median across the four models.

Two additional measures were adopted to ensure the robustness of the driver analysis. First, because macroalgal production is a component of total mariculture production, the association between the two could partly reflect a part–whole correlation. The regression was therefore repeated using Culture_ex, both in level and in first-difference (annual growth rate) form; the first-difference specification removes the mechanical part–whole link as well as common time trends. Excluding macroalgae from the mariculture total leaves the bivari-

ate association essentially unchanged (R^2 = 0.9690 vs. 0.9768 with macroalgae included), and the association persists in growth rate form (R^2 = 0.266, p = 0.034, n = 17), indicating a genuine co-movement rather than a part–whole artifact. Second, variance inflation factors (VIFs) were computed to diagnose multicollinearity. Because mariculture production and domestic water use are strongly inter-correlated (r = 0.975), the five-predictor specification exhibited substantial multicollinearity (maximum VIF ≈ 33); the MLR was accordingly simplified to the two predictors above (VIF = 3.6), which retains a high training fit (R^2 = 0.980), is formally preferred by information criteria (AIC = 33.4 vs. 36.8 and BIC = 36.1 vs. 42.2 for the five-predictor model), and improves rolling-origin out-of-sample performance (1-year RMSE = 0.82 vs. 1.25 × 10^4 t). The five-predictor MLR is retained only as a sensitivity analysis and is not used for the primary projections. Stationarity tests (ADF and KPSS) indicated that the level series are trended, and Engle–Granger tests did not support cointegration ($p \approx 0.986$); level regressions are therefore interpreted strictly as associations, with growth rate regressions serving as the primary robustness evidence.

Although macroalgal production is a component of total mariculture production, the total was retained as a predictor in the projection model for three reasons: (i) the part–whole robustness tests described above show that the association is not driven by the accounting identity; (ii) macroalgae account for only ~9% of total mariculture production (2023), so the mechanical component of the regression slope is bounded and small; and (iii) within the scenario framework, total mariculture production is an exogenous driver trajectory defined by policy assumptions, and the MLR is used for prediction rather than causal attribution.

Three management scenarios were designed for the 2023–2042 projection. Critically, all four models were trained once on the 2006–2023 historical record and their parameters were held fixed thereafter; scenario interventions were applied exclusively to the exogenous driver trajectories, never to model coefficients, so that inter-scenario differences are attributable to the driver pathways alone. Each driver trajectory follows its historical linear trend with the intercept calibrated so that the trajectory passes through its trend-fitted 2023 value, and projections are initialized at the observed 2023 production (14.60 × 10^4 t), ensuring continuity at the historical–projection boundary. Monte Carlo simulation (N = 500) with Gaussian noise around the anchored trends propagates driver uncertainty into the projections. Scenario 1 (Baseline Continuation, Business-as-Usual) assumes current trends continue without major policy changes, with environmental factors following historical linear trends plus random noise and mariculture production increasing at the historical rate of 4.79 × 10^4 t yr^{-1}; Scenario 2 (Expansion with Intervention, Active Management) assumes active policy support for mariculture expansion—including increased investment, technology promotion, and area expansion—so that mariculture production increases at an accelerated rate (9.59 × 10^4 t yr^{-1}, double the baseline slope, with the intercept recalibrated to −19,245.0 to maintain continuity at 2023) and domestic water consumption increases at a higher rate (1.21 × 10^8 m^3 yr^{-1}, double the baseline slope), reflecting urbanization and population growth; and Scenario 3 (Static Freeze, No New Investment) assumes no new investment or policy support, with mariculture production remaining at approximately the 2023 level (≈146 × 10^4 t, its trend-fitted 2023 value) with minimal growth, while industrial and domestic water consumption remain at current levels with random fluctuations.

Model predictive performance was evaluated out of sample. Cross-validation was performed primarily using rolling-origin (expanding-window) validation for all four models: models were refit on data up to each origin year and used to forecast subsequent years, yielding one-year-ahead (origins 2012–2022, n = 11) and three-year-ahead (origins 2012–2020, n = 9) forecast errors. Leave-one-out cross-validation (LOOCV) was additionally computed for the two regression models (MLR, RFR) and is reported in Section 3.3 for

completeness; because LOOCV is subject to information leakage in time-series settings, model comparison relies primarily on the rolling-origin results.

2.6. Short-Term Carbon Sequestration Accounting

Following the mass conservation boundary recommended for seaweed carbon accounting [7,42,43], total photosynthetic carbon fixation by cultivated macroalgae is partitioned into three fates: harvested biomass, particulate organic carbon (POC), and dissolved organic carbon (DOC) released during growth. We quantify short-term (annual) sequestration as the sum of these components, following the Chinese industry standard HY/T 0305—2021 [44]; long-term storage beyond the annual scale is addressed qualitatively in Section 4.6.

It should be emphasized that the carbon accounting in this study refers to short-term carbon sequestration, defined as the carbon fixed in harvestable macroalgal biomass and released as organic detritus over the cultivation cycle (annual timescales). We do not claim permanent (centennial-scale) sequestration, which requires carbon to be durably isolated from the atmosphere, e.g., through burial in marine sediments or transformation into refractory dissolved organic carbon [7,42,45]. This short-term, harvest-based accounting convention follows the established practice of mariculture carbon sink estimation in China [13,20,22] and the Chinese industry standard for marine carbon sink accounting (HY/T 0305—2021), under which carbon removed from coastal waters through harvest is recognized as a removable carbon sink.

During the cultivation cycle, the carbon fixed by macroalgae through photosynthesis has, by mass conservation, only three fates: retention in biomass that is ultimately harvested, release as particulate organic carbon (POC) through fragmentation and blade erosion, and release as dissolved organic carbon (DOC) through exudation [46]. That is,

$$C_{total} = C_{bio} + POC + DOC, \tag{1}$$

where C_{total} is total annual carbon sequestration (t C), including both harvested biomass carbon and organic debris released during growth; C_{bio} is the carbon contained in harvested biomass, with macroalgal production taken from the statistical yearbook as captured yield.

The total short-term carbon sequestration can be obtained by rescaling the measured harvest:

$$C_{total} = \frac{P \times (1 - W) \times C_C \times 10,000}{1 - \alpha - \beta} \tag{2}$$

$$C_{bio} = P \times (1 - W) \times C_C \times 10{,}000 \tag{3}$$

where C_{bio} = *annual production* × (1 − *water content*) × *carbon content* (t C); α = 0.24 and β = 0.06 are the fractions of net primary production released as DOC and POC during growth [42,46,47]; total annual sequestration is thus $C_{total} = C_{bio}/(1 - \alpha - \beta)$, i.e., detritus pathways add 42.9% beyond harvested biomass.

CO_2 equivalent was calculated using the following conversion factor:

$$CO_2 = C_{total} \times 3.67 \tag{4}$$

where 3.67 is the molecular weight ratio of CO_2 to C (44/12).

2.7. Economic Valuation

Economic valuation of carbon sequestration was conducted using the Xiangshan first-order blue carbon auction price of 106 RMB/t CO_2 (announced in 2023). This price represents the first official blue carbon trading benchmark in Zhejiang Province and provides a realistic market-based valuation anchor. We note, however, that it reflects a local auction price rather than an accessible national market price (Section 4.3). To complement

undiscounted cumulative values, we additionally report the net present value (NPV) of the Baseline-scenario value stream at discount rates of 3%, 5%, and 8%, and a sensitivity analysis across carbon prices of 50–200 RMB t^{-1} CO_2 (Section 3.5). The 3000–5000 RMB t^{-1} (wet weight) range used for product-value comparison corresponds to the range of farm-gate unit values for algae aquaculture in Zhejiang, derived as the ratio of output value to production reported in the China Fishery Statistical Yearbook [32].

$$Economic\ value = CO_{2sequestration} \times 106\ \text{RMB/t}\ CO_2 \quad (5)$$

All data processing, statistical analysis, model construction, and visualization were conducted using Python 3.12.7 with the following libraries: pandas (data manipulation), numpy (numerical computing), scipy.stats (statistical analysis), scikit-learn (machine learning), statsmodels (time series analysis), and matplotlib (visualization).

To evaluate the sensitivity of the valuation to carbon-price variation, cumulative values were additionally computed across a price range of 50–200 RMB t^{-1} CO_2, spanning observed prices in China's national carbon market, the Xiangshan auction benchmark, and international voluntary blue carbon credits. The net present value (NPV) of the Baseline cumulative revenue was calculated at discount rates of 3%, 5%, and 8%.

3. Results

3.1. Historical Trends in Macroalgal Production (2001–2023)

Zhejiang's macroalgal production exhibited a pronounced increasing trend from 2001 to 2023 (Figure 4). Production increased from 2.83 × 10^4 t (2001) to 14.60 × 10^4 t (2023), representing a 5.2-fold increase over 22 years. The growth was not uniform: a relatively stable period occurred during 2001–2016 (2.83–5.34 × 10^4 t), followed by a rapid acceleration phase during 2017–2023 (7.69–14.60 × 10^4 t), with a 1.9-fold increase in just seven years.

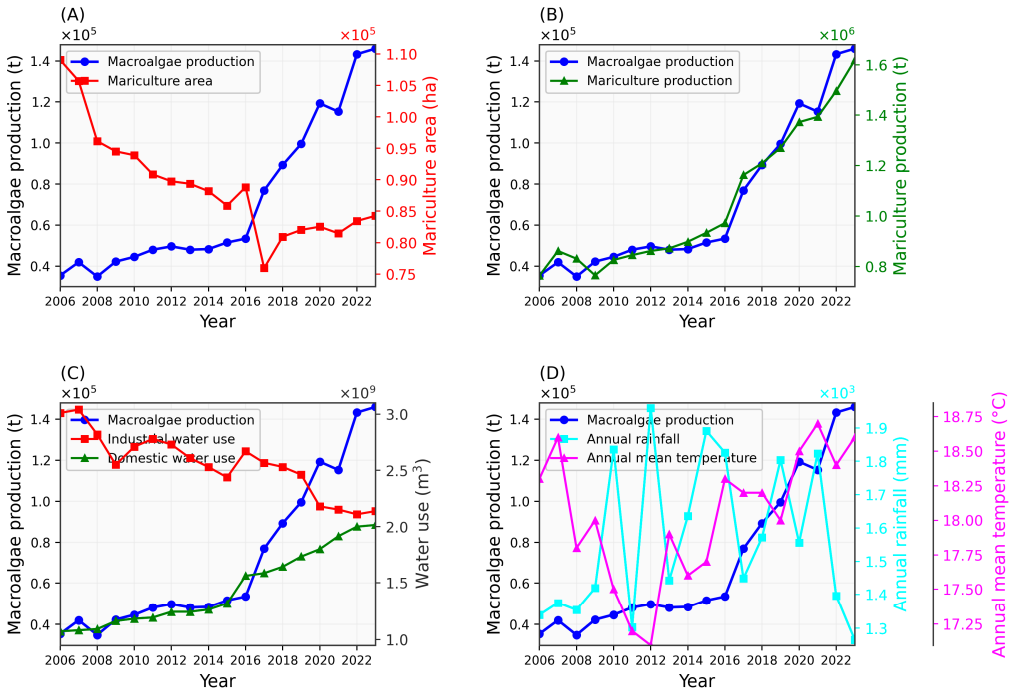


Figure 4. Changes in macroalgae production and environmental factors during 2006–2023. (**A**) Macroalgae production and mariculture area; (**B**) macroalgae production and mariculture production; (**C**) macroalgae production and industrial and domestic water use; (**D**) macroalgae production and annual rainfall and annual mean temperature.

Concurrently, total mariculture production increased from 76.32 × 10^4 t (2006) to 161.81 × 10^4 t (2023), a 2.1-fold increase. Mariculture area, however, decreased from 109.06 × 10^3 ha (2006) to 84.26 × 10^3 ha (2023), a 22.7% reduction. This divergence indicates that yield per unit area increased substantially, likely due to technological improvements, species optimization, and intensified cultivation practices.

Industrial water consumption decreased from 30.10 × 10^8 m^3 (2006) to 21.38 × 10^8 m^3 (2023), a 29.0% reduction, reflecting industrial restructuring and water conservation measures. Domestic water consumption increased steadily from 10.70 × 10^8 m^3 (2006) to 20.15 × 10^8 m^3 (2023), an 88.3% increase, consistent with urbanization and population growth. Annual rainfall and temperature showed no clear trends, with high interannual variability (rainfall coefficient of variation: 15.3%; temperature range: 17.1–18.7 °C).

3.2. Factors Associated with Macroalgal Production

Analysis of environmental factor relationships revealed significant associations between macroalgal production and environmental factors (Figure 5). Total mariculture production showed the strongest positive relationship with macroalgal yield (R^2 = 0.9768, p < 0.001). This strong relationship likely reflects the multi-trophic level integrated aquaculture system, where macroalgae benefit from nutrient cycling associated with fish and shellfish cultivation, or from shared infrastructure and management practices that promote overall aquaculture expansion.

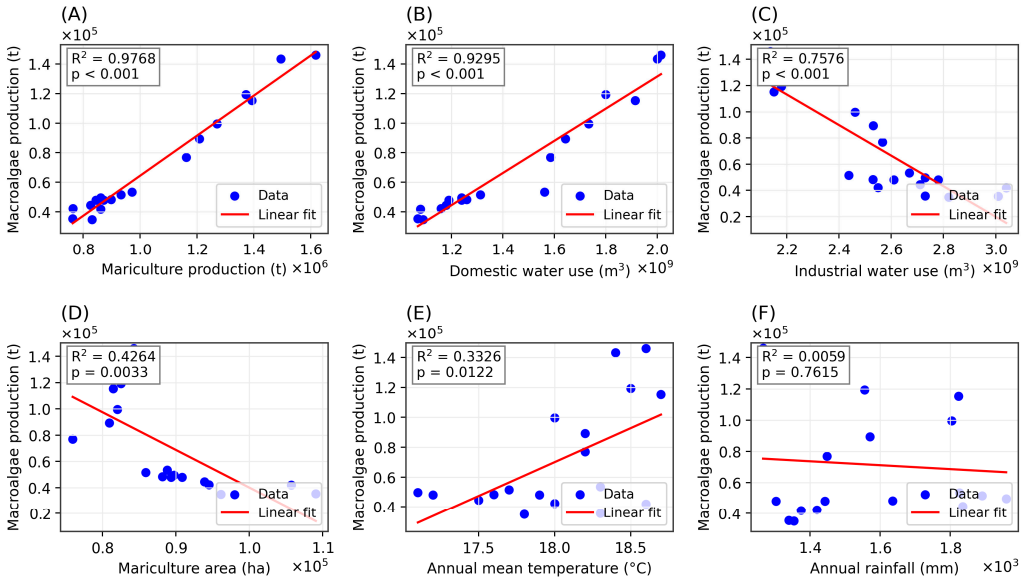


Figure 5. Relationship between macroalgal production and environmental factors during 2006–2023. (**A**) Macroalgal production versus mariculture production; (**B**) macroalgal production versus domestic water use; (**C**) macroalgal production versus industrial water use; (**D**) macroalgal production versus mariculture area; (**E**) macroalgal production versus annual mean temperature; (**F**) macroalgal production versus annual rainfall.

Because most socioeconomic variables exhibit pronounced monotonic trends over 2006–2023, we tested the stationarity of all series using Augmented Dickey–Fuller (ADF) and Kwiatkowski–Phillips–Schmidt–Shin (KPSS) tests (Table 2). Macroalgal production, total mariculture production, and industrial and domestic water use are non-stationary in levels (KPSS p < 0.05), and an Engle–Granger test found no evidence of cointegration between macroalgal and total mariculture production (p = 0.99). Level-based R^2 values are therefore reported as descriptive measures of co-movement only. To assess whether the associations survive detrending, we re-estimated them in first differences: the association

with total mariculture production persists (R^2 = 0.42, p = 0.005; R^2 = 0.30, p = 0.024 when macroalgal production is excluded from the mariculture total), whereas the associations with domestic (R^2 = 0.005, p = 0.79) and industrial water use (R^2 = 0.03, p = 0.48) do not, indicating that the latter reflect shared long-term socioeconomic trends rather than year-to-year coupling. Residual diagnostics for the projection regression showed no significant autocorrelation (Durbin–Watson = 1.50; Breusch–Godfrey p = 0.39), and coefficient significance was unchanged under Newey–West HAC standard errors ($p < 0.001$ for total mariculture production).

Table 2. Stationarity tests for the study variables (2006–2023).

Variable	ADF p (Level)	ADF p (1st diff.)	KPSS p (Level)	KPSS p (1st diff.)
Macroalgal production	0.998	0.889	0.020	0.043
Total mariculture production	0.998	0.020	0.018	0.038
Industrial water use	0.992	0.346	0.019	0.100
Domestic water use	0.993	0.003	0.016	0.100
Rainfall	0.005	0.818	0.100	0.084
Temperature	0.817	0.018	0.100	0.100

Note: ADF null hypothesis = unit root; KPSS null = stationarity. The differenced macroalgal series is dominated by the 2017 production break; at n = 18 both tests have low power and results should be read as indicative.

Domestic water consumption also exhibited a strong positive level association (R^2 = 0.9295, $p < 0.001$). However, this correlation does not survive first-differencing (R^2 = 0.005, p = 0.79), indicating that it reflects shared long-term socioeconomic trends rather than year-to-year coupling. Domestic water use is therefore interpreted strictly as a contextual proxy of coastal urbanization: it covaries with coastal population size, urbanization level, and associated economic activity, which jointly underlie both domestic water demand and mariculture market demand. A nutrient pathway—nitrogen and phosphorus inputs from domestic wastewater potentially supporting macroalgal growth—cannot be excluded but is not testable with the present data.

Industrial water consumption showed a significant negative association (R^2 = 0.7576, $p < 0.001$). This negative relationship likely reflects industrial restructuring: as industrial water consumption decreases (due to water conservation and industrial upgrading), coastal water quality improves and more area becomes available for mariculture, supporting macroalgal production growth. Alternatively, industrial wastewater discharge may contain toxic substances that inhibit macroalgal growth, or industrial zones may compete with mariculture for coastal space. This association is likewise absent in first differences (R^2 = 0.03, p = 0.48) and is interpreted as a long-run co-movement consistent with industrial restructuring, rather than a demonstrated causal mechanism.

Mariculture area exhibited a significant negative association (R^2 = 0.4264, p = 0.0033). This counterintuitive relationship reflects the policy-driven reduction in mariculture area after 2019 (from 109.06 to 84.26 $\times$ 10^3 ha), which was offset by dramatic improvements in per-unit yield (from 0.32 to 1.73 t ha^{-1}). This demonstrates that area reduction did not constrain production growth, as technological intensification compensated for spatial contraction.

Annual temperature showed a weak but significant positive association (R^2 = 0.3326, p = 0.0122). The relationship suggests that warmer temperatures within the observed range (17.1–18.7 °C) may enhance macroalgal growth, consistent with the thermal biology of subtropical species. However, the relatively weak explanatory power indicates that temperature is not the primary limiting factor for macroalgal production in Zhejiang.

Annual rainfall showed no significant association (R^2 = 0.0059, p = 0.7615). This lack of relationship suggests that either rainfall is not a limiting factor for macroalgal production, or that the high heat capacity of seawater buffers the effects of rainfall-induced temperature and salinity fluctuations.

3.3. Model Performance and Projections

Four models were trained on historical data (2006–2023) and used to project macroalgal production under three scenarios (2023–2042). In-sample goodness of fit is reported in Table 3 for transparency; predictive performance was assessed out-of-sample using rolling-origin (expanding-window) validation for all four models—one-year-ahead (origins 2012–2022, n = 11) and three-year-ahead (origins 2012–2020, n = 9)—complemented by leave-one-out cross-validation (LOOCV) for the two regression models (Table 4). Because LOOCV is subject to information leakage in time-series settings, model comparison relies primarily on the rolling-origin results. No single model is designated as primary; headline projections are reported as the ensemble median across the four models, with the inter-model range and the 80% Monte Carlo interval measuring structural and statistical uncertainty, respectively.

Table 3. In-sample goodness of fit on historical data (2006–2023).

Model	R^2 (Historical)	RMSE (Historical)	Key Features
MLR	0.980	0.52	Linear, interpretable coefficients
RFR	0.955	0.77	Non-linear, captures interactions
TSE	0.952	0.89	Trend-based, no external variables
EC-TS	0.889	1.22	Combines trend and environment

Note: In-sample R^2 and RMSE are goodness-of-fit measures on the training data and are not indicative of predictive skill; out-of-sample performance is reported in Table 4.

Table 4. Out-of-sample predictive performance: LOOCV and rolling-origin (expanding-window) validation.

Model	LOOCV Q^2	LOOCV RMSE (10^4 t)	Rolling-Origin 1-yr RMSE (10^4 t)	Rolling-Origin 3-yr RMSE (10^4 t)
MLR	0.970	0.63	0.82	1.62
RFR	0.938	0.91	1.75	3.54
TSE	—	—	1.19	2.47
EC-TS	—	—	1.11	2.13

Note: LOOCV applies to the regression models (MLR, RFR); the temporal models (TSE, EC-TS) are evaluated by rolling-origin validation only. Rolling-origin validation used an expanding training window with 11 origins (2012–2022) for the 1-year horizon and 9 origins (2012–2020) for the 3-year horizon; all models were refit at each origin, trained on all years prior to the origin year and used to predict the observation at origin + horizon − 1. LOOCV statistics are subject to information leakage in time-series settings and are shown for completeness; model comparison relies on the rolling-origin results. Dash (—): not applicable.

All models fit the historical series well ($R^2 \geq 0.889$; Table 3). The two-predictor MLR achieved R^2 = 0.980 (adjusted R^2 = 0.977) with RMSE = 0.52 × 10^4 t and was preferred over the five-predictor specification on parsimony grounds (AIC 33.4 vs. 36.8; BIC 36.1 vs. 42.2). RFR, despite its depth-constrained configuration, achieved R^2 = 0.955 with RMSE = 0.77 × 10^4 t; with only 18 observations, such in-sample statistics are uninformative about predictive skill (Table 4). Time Series Extrapolation (TSE) achieved R^2 = 0.952 with RMSE = 0.89, capturing the underlying growth trend but lacking responsiveness to

environmental change. The Environmentally Constrained Time Series (EC-TS) model, with data-derived sigmoid centers (historical means: mariculture 105.3 × 10^4 t, industrial water 25.6 × 10^8 m^3, domestic water 14.5 × 10^8 m^3), achieved R^2 = 0.889 and RMSE = 1.22.

Out-of-sample validation (Table 4) confirmed useful predictive skill while revealing the expected gap between in-sample fit and forecast accuracy. Under rolling-origin validation, one-year-ahead RMSE ranged from 0.82 (MLR) to 1.75 × 10^4 t (RFR), and three-year-ahead RMSE from 1.62 (MLR) to 3.54 × 10^4 t (RFR); relative to 2023 production (14.60 × 10^4 t), these correspond to typical errors of roughly 6–24%. LOOCV statistics for the regression models (MLR Q^2 = 0.970, RMSE = 0.63; RFR Q^2 = 0.938, RMSE = 0.91 × 10^4 t) are reported for completeness but are optimistic owing to the information leakage inherent in leave-one-out schemes for autocorrelated series. MLR achieved the lowest rolling-origin error at both horizons, followed by EC-TS and TSE, while RFR showed the largest forecast errors because tree-based predictions cannot extrapolate beyond the training domain. The five-predictor MLR sensitivity specification (1-year RMSE = 1.25; 3-year RMSE = 1.98 × 10^4 t) also underperformed the parsimonious two-predictor MLR. These results motivate reporting all projections as ensemble medians rather than relying on any single model.

Figures 6–8 show the projected macroalgal production trajectories under the three scenarios using four modeling approaches. Under the Baseline scenario (Figure 6A), EC-TS projected the strongest growth, from 14.60 × 10^4 t (2023) to 76.7 × 10^4 t (2042), reflecting the compounding effect of favorable environmental suitability scores on the underlying growth trend. TSE projected moderate growth to 37.8 × 10^4 t, while MLR and RFR produced more conservative estimates of 25.2 and 13.3 × 10^4 t, respectively. The ensemble median reaches 31.5 × 10^4 t by 2042 (80% Monte Carlo interval 31.3–31.8 × 10^4 t). The divergence between EC-TS/TSE and MLR/RFR after 2030 highlights the critical role of environmental trend assumptions in long-term projections.

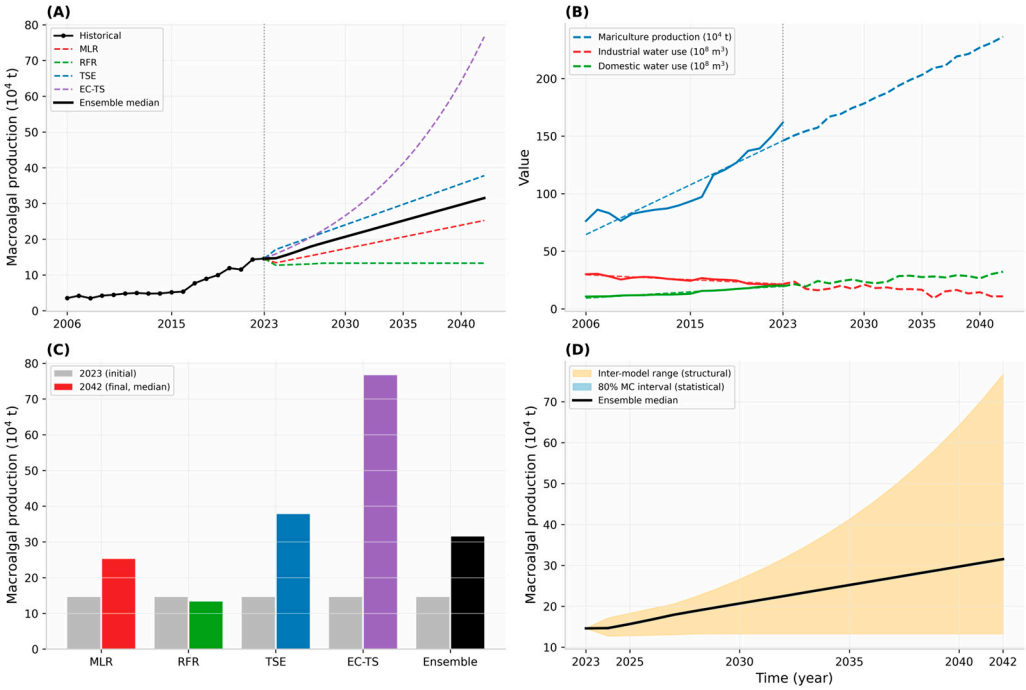


Figure 6. Scenario 1 (Baseline Continuation): (**A**) projected production trajectories by model; (**B**) driver trajectories; (**C**) comparison of 2023 and 2042 projections; (**D**) ensemble median with inter-model range and 80% Monte Carlo interval.

Under the Expansion scenario (Figure 7A), which simulates the doubling of the mariculture growth rate through active policy intervention, the ensemble median reaches

37.1 × 10^4 t by 2042 (+17.8% relative to Baseline). EC-TS again produced the highest projection (77.0 × 10^4 t), followed by TSE (37.8 × 10^4 t) and MLR (36.4 × 10^4 t), while RFR remained at 13.3 × 10^4 t owing to its inability to extrapolate beyond the training domain. All trajectories are continuous at the 2023 boundary because scenario driver trajectories are anchored to their trend-fitted 2023 values and model parameters are held fixed (Section 2.5). We note that Expansion scenario driver values exceed the historical calibration range in later years; so, single-model projections under this scenario—particularly MLR, whose linear response is unbounded—should be interpreted with caution. The ensemble median is the preferred estimator.

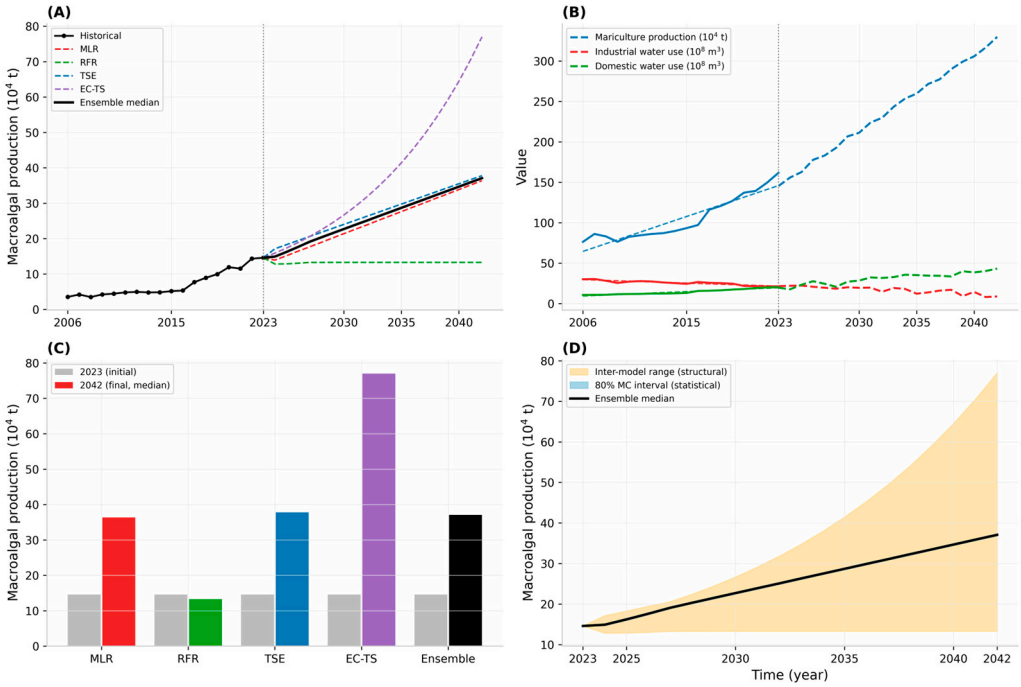


Figure 7. Scenario 2 (Expansion with Intervention): (**A**) projected production trajectories by model; (**B**) driver trajectories; (**C**) comparison of 2023 and 2042 projections; (**D**) ensemble median with inter-model range and 80% Monte Carlo interval.

Under the Static scenario (Figure 8A), which assumes production stagnation due to lack of new investment, the ensemble median reaches only 25.2 × 10^4 t by 2042 (−20.0% relative to Baseline). EC-TS projected 67.4 × 10^4 t and TSE 37.8 × 10^4 t (identical across scenarios because it ignores environmental inputs), while MLR and RFR converged at 12.4 and 11.8 × 10^4 t, respectively. The comparison of 2023 versus 2042 projections across all methods (Figures 6C, 7C and 8C) shows that EC-TS consistently produces the highest estimates when environmental trends are favorable, whereas RFR consistently yields the lowest due to its regression-to-mean behavior beyond the training domain.

The environmental factor trajectories underlying these projections (Figures 6B, 7B and 8B) reveal the sources of scenario divergence. Under the Baseline scenario, total mariculture production continues its historical upward trend, rising from 161.8 × 10^4 t (2023) to approximately 237.2 × 10^4 t (2042), while industrial water use gradually declines (to 12.4 × 10^8 m^3) and domestic water use steadily increases (to 31.2 × 10^8 m^3). The Expansion scenario accelerates mariculture growth to 327.6 × 10^4 t by 2042 (with domestic water use reaching 42.7 × 10^8 m^3), whereas the Static scenario holds mariculture production near its 2023 trend level (≈146 × 10^4 t). These divergent driver trajectories are directly translated into suitability scores by the EC-TS model: the Expansion scenario maintains

high cultivation suitability (culture score > 0.95), while the Static scenario shows declining suitability as industrial constraints intensify.

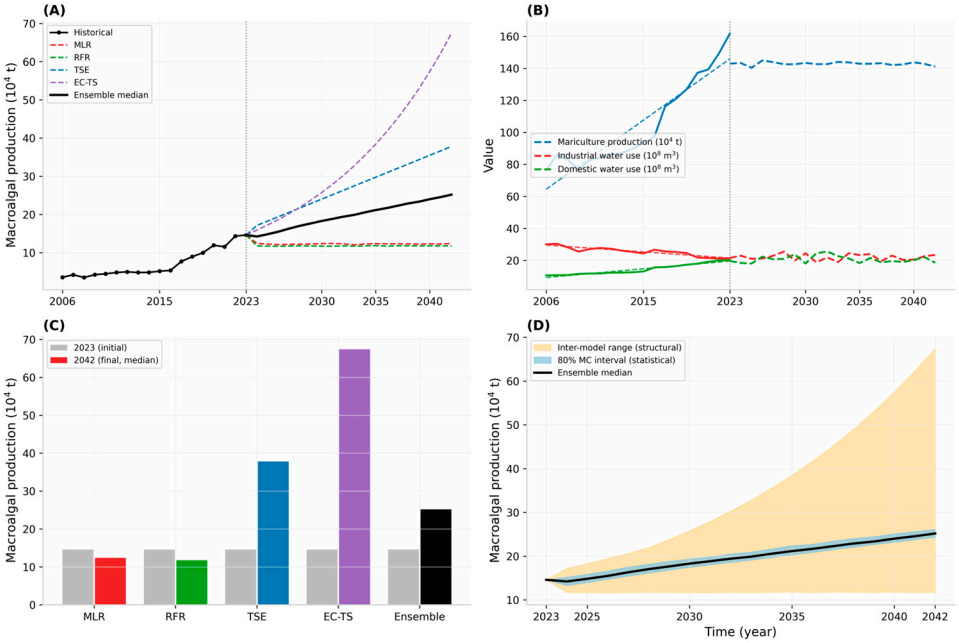


Figure 8. Scenario 3 (Static Freeze): (**A**) projected production trajectories by model; (**B**) driver trajectories; (**C**) comparison of 2023 and 2042 projections; (**D**) ensemble median with inter-model range and 80% Monte Carlo interval.

The multi-method prediction uncertainty ranges (Figures 6D, 7D and 8D) quantify the uncertainty envelope for each scenario. By 2042, the inter-model (structural) range spans 13.3–76.7 $\times$ 10^4 t under the Baseline scenario (ensemble median 31.5 $\times$ 10^4 t), 13.3–77.0 $\times$ 10^4 t under Expansion (median 37.1 $\times$ 10^4 t), and 11.8–67.4 $\times$ 10^4 t under Static (median 25.2 $\times$ 10^4 t). In contrast, the 80% Monte Carlo intervals around the ensemble medians are narrow (e.g., 31.3–31.8 $\times$ 10^4 t for the Baseline 2042 projection), indicating that statistical (parameter) uncertainty is small relative to structural uncertainty. These results underscore the importance of ensemble approaches in macroalgal production forecasting, as single-model projections may introduce substantial bias depending on model structure and scenario assumptions.

3.4. Carbon Sequestration Assessment (2006–2023)

We applied the weighted average carbon content (27.25% DW) derived from species-specific values reported in Table 1, together with water content (~85%) and the DOC/POC release fractions defined in Section 2.6, to convert production into carbon sequestration (Section 2.6). Over 2006–2023, annual carbon sequestration averaged 4176 t C (15,327 t CO_2 equivalent), rising from 2067 t C in 2006 to 8525 t C in 2023. The cumulative sequestration over this 18-year period amounted to 75,175 t C (275,892 t CO_2 equivalent). Monetized at the Xiangshan first-order blue carbon auction price (106 RMB t^{-1} CO_2), the annual sequestration value averaged 1.625 $\times$ 10^6 RMB, with a cumulative value of 2.92 $\times$ 10^7 RMB (Figure 9A).

Notably, carbon sequestration accelerated dramatically after 2017, reflecting the production boom. In 2023 alone, carbon sequestration reached 8525 t C (31,288 t CO_2 equivalent), with an estimated value of 3.32 $\times$ 10^6 RMB—more than four times the 2006 level (2067 t C).

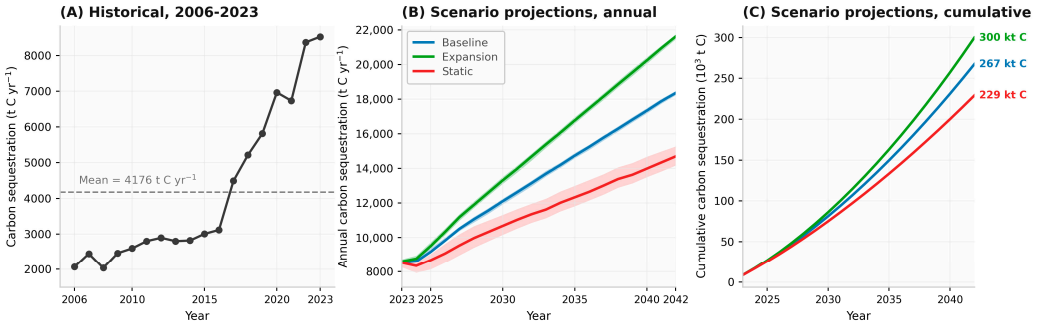


Figure 9. Historical and projected carbon sequestration by macroalgal mariculture in Zhejiang. (**A**) Annual carbon sequestration during 2006–2023 (t C yr^{-1}), with the dashed line indicating the 18-year mean (4176 t C yr^{-1}); (**B**) projected annual carbon sequestration under the three scenarios (2023–2042, ensemble median; shaded bands denote the 80% Monte Carlo interval); (**C**) cumulative carbon sequestration over 2023–2042, with end-point labels (thousand t C).

3.5. Scenario-Based Carbon Sequestration Projection (2023–2042)

Across the 2023–2042 projection horizon, the three scenarios yield markedly different cumulative carbon sequestration outcomes (Table 5; Figure 9B,C). Under the Baseline scenario, cumulative sequestration reaches 267,246 t C (980,792 t CO_2 equivalent), with a cumulative value of 1.04×10^8 RMB at 106 RMB t^{-1} CO_2. The Expansion scenario increases cumulative sequestration by 12.1% relative to the Baseline (299,511 t C; 1,099,205 t CO_2; 1.17×10^8 RMB), whereas the Static scenario reduces it by 14.3% (229,010 t C; 840,467 t CO_2; 8.91×10^7 RMB). Discounted at 3%, 5%, and 8%, the net present value of the Baseline carbon revenue stream is 0.77×10^8, 0.64×10^8, and 0.50×10^8 RMB, respectively. The sensitivity of the cumulative value to carbon price is summarized in Table 6.

Table 5. Summary of scenario projections (2023–2042, ensemble median).

Scenario	Cumulative C (t C)	Cumulative CO_2 (t CO_2)	Cumulative Value (10^8 RMB)	2042 Production (10^4 t)	Δ vs. Baseline (%)
Baseline Continuation	267,246	980,792	1.04	31.5	—
Expansion with Intervention	299,511	1,099,205	1.17	37.1	+12.1
Static Freeze	229,010	840,467	0.89	25.2	−14.3

Table 6. Sensitivity of cumulative carbon value (2023–2042, Baseline scenario) to carbon price.

Carbon Price (RMB t^{-1} CO_2)	Cumulative Value (10^8 RMB)	Share of Product Value (%)
50	0.49	0.21–0.36
80	0.78	0.34–0.57
106 (auction price)	1.04	0.45–0.76
150	1.47	0.64–1.08
200	1.96	0.85–1.43

Note: Assuming a macroalgal product price of 3000–5000 RMB t^{-1}. The NPV of the Baseline cumulative value at 106 RMB t^{-1} CO_2 is 0.7654, 0.6367, and 0.4968 $\times$ 10^8 RMB at discount rates of 3%, 5%, and 8%, respectively.

The annual economic value under the Baseline scenario averages 5.20×10^6 RMB yr^{-1}, representing approximately 0.45–0.76% of the estimated direct aquaculture product value

of macroalgal production (at 3000–5000 RMB t^{-1} wet weight [32]). Carbon revenue alone therefore constitutes only a marginal supplement to product income, underscoring the need for diversified benefit mechanisms (Section 4.3).

A sensitivity analysis across carbon prices of 50–200 RMB t^{-1} CO_2 shows that the cumulative Baseline value ranges from 0.49×10^8 to 1.96×10^8 RMB (Table 6). Even under the most optimistic price assumption, carbon-credit revenue remains below approximately 1.5% of the direct aquaculture product value. Because a simple sum of nominal annual values has no clear economic meaning over a two-decade horizon, we additionally report the net present value (NPV) of the Baseline revenue stream: 0.77, 0.64, and 0.50×10^8 RMB at discount rates of 3%, 5%, and 8%, respectively (Table 6, note); the undiscounted cumulative sums reported above are retained only as indicators of physical scale. These results confirm that the study's economic conclusions are not contingent on the single 106 RMB t^{-1} CO_2 benchmark.

4. Discussion

4.1. Environmental Correlates and Carbon Sequestration Context

Regression analysis reveals a clear ranking of associations: total mariculture production (R^2 = 0.9768) > domestic water consumption (R^2 = 0.9295) > industrial water consumption (R^2 = 0.7576) > mariculture area (R^2 = 0.4264) > annual temperature (R^2 = 0.3326) > annual rainfall (R^2 = 0.0059). This ranking indicates that macroalgal production is primarily associated with anthropogenic factors linked to coastal economic activity, rather than climatic variables. The dominance of total mariculture production aligns with the Integrated Multi-Trophic Aquaculture paradigm, where macroalgae occupy the nutrient-assimilating trophic layer within multi-species cultivation systems [23,24]. Domestic water consumption likely proxies for coastal population growth, which may increase wastewater nutrient discharge and seafood market demand [48]. The negative association with industrial water consumption may reflect industrial–mariculture competition for coastal space and water quality, consistent with the "green transition" hypothesis that industrial upgrading can simultaneously reduce pollution and enhance blue carbon ecosystems [28]. It should be noted, however, that these bivariate R^2 values partly reflect common trending behavior among non-stationary series (e.g., r = 0.975 between total mariculture production and domestic water consumption; Sections 2.5 and 3.2) and therefore indicate co-movement rather than confirmed causation.

To contextualize the carbon sequestration potential of macroalgal mariculture, we compared our estimates with other blue carbon ecosystems (Table 7). Zhejiang's macroalgal carbon sequestration rate (584.25 t C per 10^4 t of macroalgae, combining harvested biomass and released detritus) is comparable to areal sequestration rates reported for natural blue carbon habitats. Fourqurean et al. [49] estimated global mean sequestration rates of 226 ± 39 g C m^{-2} yr^{-1} for mangroves, 138 ± 21 g C m^{-2} yr^{-1} for seagrass beds, and 218 ± 24 g C m^{-2} yr^{-1} for salt marshes. At the cultivation density of Zhejiang (approximately 1000 ha per 10^4 t production), the areal sequestration rate converts to approximately 584 kg C ha^{-1} yr^{-1}. This is lower than the global mean carbon accumulation rate of 2447 kg C ha^{-1} yr^{-1} [50] for coastal marsh sediments, an expected difference because the macroalgal carbon quantified here is realized through harvest removal and detrital release rather than long-term sediment burial [7,51]. Nevertheless, the high biomass productivity of cultivated macroalgae—achieved through optimized species selection, nutrient enrichment, and reduced herbivory pressure [6,15]—allows this flux to be delivered over large, actively managed areas without requiring habitat restoration.

Table 7. Comparison of areal carbon sequestration rates across blue carbon ecosystems.

Ecosystem	Areal Carbon Sequestration Rate (kg C ha^{-1} yr^{-1})	Source
Macroalgal mariculture (Zhejiang, this study)	584	This study
Mangroves (global mean)	2260 ± 390	[49]
Salt marshes (global mean)	2180 ± 240	[49]
Seagrass beds (global mean)	1380 ± 210	[49]
Coastal marsh sediments (global mean)	2447	[50]

At the national scale, Tang et al. [22] estimated that China's shellfish and seaweed mariculture takes up 3.79 ± 0.37 Mt C yr^{-1}, while national-scale estimates range from 0.28 Tg C yr^{-1} using the carbon sink conversion rate of 5.20%. Our provincial estimate of 4176 t C yr^{-1} (2006–2023 average) represents approximately 0.11–1.49% of these national estimates, which is consistent with Zhejiang's contribution of 4.5–8.3% to China's total macroalgal production [12]. The divergence between our estimate and the national-scale values primarily arises from different carbon accounting boundaries: we include only harvestable biomass and readily measurable detritus, whereas national estimates often incorporate speculative contributions from carbon export to deep-sea sediments [51].

The relatively low R^2 values for temperature (0.3326) and rainfall (0.0059) suggest that, within the observed range (17.1–18.7 °C, 1200–2000 mm), climatic variability is not the primary limiting factor for macroalgal production in Zhejiang. This climatic buffering likely reflects the adaptability of subtropical macroalgal species to variable conditions and the moderating effect of coastal water heat capacity on temperature fluctuations [25]. However, this does not imply climate change immunity: extreme events (marine heatwaves, typhoons) and long-term trends (ocean warming, acidification) may exert impacts beyond the current observational envelope [52,53]. The "area reduction, yield increase" pattern—22.7% decrease in mariculture area coinciding with 4.1-fold production increase—is consistent with successful technological intensification through deep-sea cultivation expansion and high-yielding variety promotion, a trend that is expected to continue under favorable policy conditions.

4.2. Comparison with Previous Studies

Previous estimates of Zhejiang's average annual macroalgal carbon sequestration were approximately 1.03×10^4 t C during 1999–2012, based on species-specific carbon contents and harvest production data. Our updated estimate for 2006–2023 averages 4176 t C yr^{-1}. This substantial difference arises from three factors: (1) inclusion of organic detritus carbon (POC + DOC), which contributes an additional 42.9% beyond harvested biomass based on updated DOC release estimates [46] (i.e., total sequestration = harvested carbon ÷ (1 − 0.24 − 0.06) = 1.429 × harvested carbon); (2) our analysis captures the recent production boom (2017–2023), during which single-year sequestration reached 8525 t C in 2023; and (3) methodological improvements in carbon accounting that incorporate refractory dissolved organic carbon pathways [7,54]. The 2023 sequestration alone (8525 t C) illustrates the dramatic growth of Zhejiang's macroalgal industry.

Yue et al. [21] estimated that Zhejiang contributes 33–46% of China's total macroalgal carbon sink increment potential, with a projected 2022–2027 carbon sequestration of 367,892.84 t CO_2 yr^{-1} (approximately 100,243 t C yr^{-1}). Our Baseline scenario projects an annual average of 13,362 t C (49,040 t CO_2) for 2023–2042, which is 7.5 times lower than Yue et al.'s estimate. This divergence reflects fundamental differences in scope: Yue et al. assessed "Expandable Aquaculture Area" potential based on theoretical carrying

capacity, whereas our study estimates production-constrained sequestration under realistic environmental and policy trajectories. Additionally, Yue et al. used a higher carbon content for Porphyra (41.96% vs. our 27.35% from Table 1), which would inflate sequestration estimates by approximately 50% given Porphyra's dominance in Zhejiang's production (reported at 83% by Yue et al.). Our adoption of 27.25% DW, derived from multiple species-specific analyses, represents a more conservative and regionally calibrated parameter. The inclusion of POC and DOC detritus carbon (42.9% additional) partially bridges the gap between harvest-based and theoretical estimates, suggesting that actual sequestration likely falls between our production-constrained estimate and Yue et al.'s area-potential estimate.

Zhang et al. [13] estimated China's total macroalgal carbon sequestration at millions of tonnes annually. At the provincial scale, Zhejiang's contribution (8525 t C in 2023) represents a small but growing fraction of national totals. The increasing trend suggests that Zhejiang's share of national macroalgal carbon sequestration may be rising.

4.3. Scenario Implications and Policy Recommendations

The multi-scenario projections reveal substantial divergence in model behavior that illuminates both methodological strengths and limitations. The EC-TS model consistently produces the highest projections across all scenarios because its environmental suitability scoring mechanism compounds favorable trends: when mariculture totals rise and industrial water declines, the combined suitability score amplifies the baseline growth rate through multiplicative interaction. This amplification explains why the EC-TS 2042 projections (67.4–77.0 $\times$ 10^4 t) represent an upper bound rather than a central estimate, and we therefore report ensemble medians rather than any single model's output [14].

The RFR model's consistently conservative projections (11.8–13.3 $\times$ 10^4 t across scenarios) reflect its inherent regression-to-mean behavior: as input variables diverge from training data ranges, tree-based ensemble predictions converge toward the historical mean, effectively capping extrapolation. While this conservatism limits RFR's utility for long-range forecasting, it provides a valuable lower-bound reference that guards against overestimation. The model-dependent uncertainty ranges (Figures 6D, 7D and 8D) demonstrate that aggregation across structurally diverse models—summarized by the ensemble median—is essential for robust projection: the 2042 Baseline scenario ranges from 13.3 (RFR) to 76.7 (EC-TS) $\times$ 10^4 t, a 5.8-fold difference that underscores the hazard of relying on single-model forecasts for policy planning. We therefore adopt the ensemble median (31.5 $\times$ 10^4 t under the Baseline scenario) as the central projection throughout this study.

The Expansion scenario demonstrates that active policy support—including high-yielding strain breeding, deep-sea cultivation expansion, Integrated Multi-Trophic Aquaculture demonstration, and post-harvest market development—could raise cumulative sequestration by 12.1% over 2023–2042 relative to the Baseline trajectory. Integrating macroalgal blue carbon into provincial carbon neutrality accounting and establishing standardized monitoring, reporting, and verification protocols [43] compatible with national China Certified Emission Reduction mechanisms are essential next steps. Our transferable methodological framework combining statistical driver analysis and multi-model ensemble projection can be applied to other macroalgal-producing provinces to construct a comprehensive national blue carbon inventory [22,45].

Recent institutional developments strengthen the practical relevance of these projections. China's national voluntary greenhouse gas emission reduction trading (CCER) market was relaunched in January 2024 under the Measures for the Administration of Voluntary Greenhouse Gas Emission Reduction Trading (Trial) issued in October 2023 [30], and the first batch of approved methodologies includes coastal blue carbon projects—currently limited to mangrove restoration. Although no approved methodology yet covers

macroalgal mariculture, the national industry standard HY/T 0305—2021 [44] already provides a carbon-stock-variation accounting framework for maricultural seaweeds, offering a technical basis for future methodology development. Two practical barriers remain: (i) monitoring, reporting, and verification (MRV) costs for dispersed smallholder raft systems can exceed the carbon revenue itself at current price levels; and (ii) the prices observed in regional pilots (106 RMB t^{-1} CO_2 at the Xiangshan first-order auction; approximately 100 RMB t^{-1} CO_2 in Shengsi) derive from one-off local auctions and may not represent future CCER market clearing prices. Our valuation should therefore be read as an order-of-magnitude estimate under current pilot conditions rather than a forecast of tradable revenue.

4.4. Model Validation and Predictive Performance

Cross-validation was performed primarily using rolling-origin (expanding-window) out-of-sample validation, applied identically to all four models at 1-year and 3-year horizons (Table 4); leave-one-out cross-validation results for the regression models are also reported in Table 4 for completeness, although LOOCV is subject to information leakage in time-series settings and is therefore not used as the primary basis for model comparison. The simplified two-predictor MLR achieved the best out-of-sample performance (1-year RMSE = 0.82; 3-year RMSE = 1.62 × 10^4 t), followed by EC-TS (1.11; 2.13 × 10^4 t), whose environmental responsiveness nevertheless makes it valuable for discriminating among management scenarios. Although RFR achieved a high in-sample R^2 (0.955 under the constrained specification), its leave-one-out cross-validated Q^2 (0.938, versus 0.970 for MLR) and its rolling-origin out-of-sample errors (RMSE 1.75 and 3.54 × 10^4 t at 1- and 3-year horizons, the highest of the four models) indicate that its apparent in-sample advantage partly reflects memorization of the 18-observation training set rather than generalizable predictive skill, consistent with its known inability to extrapolate beyond the training domain (Section 2.5). The validation also reveals that all models struggle to capture the 2017 production inflection point, underscoring the inherent difficulty of predicting structural breaks. Accordingly, the multi-model ensemble median was used for the primary projections, and projections to 2042 should be interpreted as scenario-based extrapolations conditional on the assumed driver trajectories, rather than unconditional forecasts.

4.5. Addressing the Knowledge Gaps

This study was designed around four knowledge gaps identified in the Introduction Section. First, regarding the scarcity of updated province-scale assessments, we provide a 2006–2023 reassessment for Zhejiang that incorporates the post-2017 production boom and a refined, regionally calibrated carbon accounting chain (weighted carbon content 27.25% DW; DOC/POC release fractions of 0.24/0.06), yielding an annual mean of 4176 t C and a 2023 value of 8525 t C—substantially revising earlier estimates based on pre-2012 data.

Second, regarding environmental regulatory mechanisms, the combined bivariate, multivariate, and stationarity analyses show that macroalgal production co-varies most strongly with anthropogenic drivers (total mariculture production, R^2 = 0.9768; domestic water use, R^2 = 0.9295) and only weakly with climatic variables (rainfall R^2 = 0.0059), while first-difference regressions confirm a genuine short-run response to mariculture expansion (R^2 = 0.42, p = 0.005). This provides the quantitative driver hierarchy that was previously missing at the provincial scale.

Third, regarding multi-scenario projection, we demonstrate a replicable framework in which four structurally distinct models—trained once on 2006–2023 data and then held fixed—are driven by exogenous scenario trajectories, with ensemble medians and Monte Carlo intervals replacing single-model point forecasts. This design avoids the coefficient

retrospection problem of earlier practice and is consistent with emerging machine learning applications in marine carbon sink projection [26,27], while the rolling-origin evaluation makes the limits of predictability explicit (3-year-ahead RMSE of 1.62–3.54 $\times$ 10^4 t).

Fourth, regarding economic valuation, we monetize sequestration at an observed market transaction price (106 RMB t^{-1} CO_2, Xiangshan first-order blue carbon auction) rather than a theoretical shadow price, and show that carbon revenue amounts to only 0.45–0.76% of product value—evidence that blue carbon credits alone cannot currently incentivize expansion and should be bundled with ecological compensation and green-finance instruments (Section 4.3).

4.6. Uncertainties and Limitations

The weighted average carbon content (27.25% DW) adopted in this study represents a deliberate methodological choice to balance representativeness and conservatism. This value, derived from multiple species-specific analyses, falls within the reported range for commercially cultivated macroalgae in East Asian temperate waters (24–32% DW; [7,14]) but is substantially lower than Yue et al.'s [21] estimate of 41.96% for Porphyra. This divergence introduces a parameter uncertainty of CV = 21.7%, which propagates linearly into sequestration estimates. If Yue et al.'s higher carbon content was applied, our annual sequestration estimates would increase by approximately 54%, underscoring the sensitivity of carbon accounting to this critical parameter. The species ratio used may not reflect recent composition changes, as Yue et al. [21] reported Porphyra dominance has increased to 83% in Zhejiang, potentially warranting future updates to the weighted average.

Second, the analysis is correlational in nature. Although we screened drivers with a stationarity battery and first-difference regressions (Section 3.2), the 18-year annual series limits statistical power, and the associations identified—particularly the strong bivariate correlations with trending socioeconomic variables—should not be interpreted as established causal effects. The provincial-scale aggregation further masks spatial heterogeneity among mariculture zones (Xiangshan Harbor, Sanmen Bay, Zhoushan), limiting precision management support.

In addition, projections under the Expansion scenario involve driver values beyond the historical calibration range in later years; single-model projections in this region are extrapolative and assumption-driven, which further motivates the use of the ensemble median as the primary projection and the reporting of inter-model spread as structural uncertainty.

The wide ranges for POC release (9.02–70%) and DOC release (<5% to >40% [46,47]) introduce substantial uncertainty into carbon sequestration estimates. The actual long-term sequestration depends on the fraction of released carbon permanently buried or stored as refractory dissolved organic carbon, which is highly variable across local hydrodynamic conditions [42]. Moreover, our DOC/POC fractions derive from short-term decomposition experiments; whether the released carbon remains sequestered on centennial timescales—the standard relevant for carbon crediting—remains unresolved and warrants isotope-tracing and sediment burial studies.

The 2023–2042 projections extrapolate driver trajectories beyond the observed range. Driver values are anchored to trend-fitted 2023 levels and follow exogenous scenario paths, so the projections are conditional on those paths being realized; unforeseen policy shifts, extreme climate events, disease outbreaks, or market shocks could substantially alter trajectories. The inter-model spread (5.8-fold by 2042) and the widening Monte Carlo intervals (Figures 6D, 7D and 8D) partially quantify this uncertainty, but structural uncertainties—such as changes in species composition, cultivation technology, or carbon accounting rules—are not captured and should be revisited as new data become available.

Several statistical limitations should be noted. The study series are short (n = 18) and mostly non-stationary, with pronounced monotonic trends; unit-root and cointegration tests at this sample size have low power, and the 2017 production break further complicates inference. No cointegration was detected between macroalgal production and its predictors (Engle–Granger p = 0.99), so all level-based correlations are treated as descriptive co-movements, and the projection regression is used as an empirically validated mapping rather than a causal or long-run equilibrium model. More broadly, our driver analysis is correlational: statistical association cannot be equated with causation, and causal identification of the underlying mechanisms would require spatially resolved (bay- or farm-level) panel data, longer time series, or natural experiment designs.

Finally, an acknowledged limitation of this study is that the economic valuation is restricted to gross carbon-credit revenue and does not account for cultivation, MRV, transaction, or sea-area opportunity costs. These costs would reduce net benefits and are likely to vary considerably among farming systems and sites; a full net-benefit assessment will therefore require farm-level cost data that are not currently available at the provincial scale. Within the present scope, however, because the estimated carbon revenue equals only 0.45–0.76% of the direct product value (Table 6), including these costs would further reduce net benefits and would therefore reinforce the qualitative conclusion that carbon credits alone provide a weak incentive for expansion.

5. Conclusions

This study assessed the carbon sequestration capacity and future potential of macroalgal mariculture in Zhejiang Province using integrated statistical analysis and multi-model prediction. Zhejiang's macroalgal production has entered a rapid growth phase, increasing from 2.83×10^4 t (2001) to 14.60×10^4 t (2023), with total mariculture production identified as the factor most strongly associated with production (R^2 = 0.9768). Annual carbon sequestration averaged 4176 t C (15,327 t CO_2 equivalent) during 2006–2023, with cumulative sequestration reaching 75,175 t C.

Under the Baseline scenario, total carbon sequestration during 2023–2042 is projected at approximately 2.67×10^5 t C, with a cumulative economic value of ~1.04×10^8 RMB at 106 RMB/t CO_2. The multi-method prediction ranges ($11.8–77.0 \times 10^4$ t across scenarios) highlight substantial model-dependent uncertainty, underscoring the need for ensemble approaches in long-term projections. Policy interventions that double mariculture growth could raise cumulative sequestration by 12.1%, whereas stagnation would reduce it by 14.3% relative to the Baseline.

This study provides a transferable methodological framework for provincial-scale blue carbon assessment, integrating statistical analysis, machine learning prediction, and economic valuation. The findings support the integration of macroalgal blue carbon into provincial carbon neutrality accounting, while highlighting priorities for future research: direct measurement of species-specific carbon contents, bay-scale assessment to capture spatial heterogeneity, and field validation of POC/DOC release rates to reduce sequestration uncertainty.

Author Contributions: Conceptualization, T.W. and G.G.; methodology, T.W. and G.G.; software, T.W.; validation, X.X. and S.Y.; formal analysis, T.W.; investigation, L.S.; resources, Y.X. and B.L.; data curation, T.W.; writing—original draft preparation, T.W.; writing—review and editing, G.G.; visualization, T.W.; supervision, G.G.; project administration, G.G. All authors have read and agreed to the published version of the manuscript.

Funding: This work was supported by the International Cooperation Seed Funding Project for China's Ocean Decade Actions (GHZZ3702840002024020000020) and the Open Project of Key Laboratory of Marine Environmental Survey Technology and Application, Ministry of Natural Resources, P.R. China (MESTA-2024-A001).

Institutional Review Board Statement: Not applicable.

Informed Consent Statement: Not applicable.

Data Availability Statement: The data that support the findings of this study are available from the Zhejiang Statistical Yearbook and China Fishery Statistical Yearbook. Restrictions apply to the availability of these data, which were used under license for this study. The processed panel data and prediction results are available from the corresponding author upon reasonable request.

Acknowledgments: The authors thank the Zhejiang Provincial Bureau of Statistics and the Ministry of Agriculture and Rural Affairs of China for providing access to the statistical yearbooks. We also thank the reviewers for their constructive comments.

Conflicts of Interest: Authors Li Song, Yue Xu, Bo Lin, Xuexi Xiao and Saixia Ying were employed by the company Zhejiang Zhongyi Testing Research Institute Co., Ltd. The remaining authors declare that the research was conducted in the absence of any commercial or financial relationships that could be construed as a potential conflict of interest.

Abbreviations

The following abbreviations are used in this manuscript:

DOC	Dissolved Organic Carbon
POC	Particulate Organic Carbon
NPP	Net Primary Production
MLR	Multiple Linear Regression
RFR	Random Forest Regression
TSE	Time Series Extrapolation
EC-TS	Environmentally Constrained Time Series
RMSE	Root Mean Square Error
DW	Dry Weight
IMTA	Integrated Multi-Trophic Aquaculture
CV	Coefficient of Variation

References

1. Sabine, C.L.; Feely, R.A.; Gruber, N.; Key, R.M.; Lee, K.; Bullister, J.L.; Wanninkhof, R.; Wong, C.S.; Wallace, D.W.R.; Tilbrook, B.; et al. The Oceanic Sink for Anthropogenic CO_2. *Science* **2004**, *305*, 367–371. [CrossRef] [PubMed]
2. Nellemann, C.; Corcoran, E.; Duarte, C.M.; Valdés, L.; De Young, C.; Fonseca, L.; Grimsditch, G. *Blue Carbon: The Role of Healthy Oceans in Binding Carbon*; UNEP: Arendal, Norway, 2009.
3. McLeod, E.; Chmura, G.L.; Bouillon, S.; Salm, R.; Björk, M.; Duarte, C.M.; Lovelock, C.E.; Schlesinger, W.H.; Silliman, B.R. A Blueprint for Blue Carbon: Toward an Improved Understanding of the Role of Vegetated Coastal Habitats in Sequestering CO_2. *Front. Ecol. Environ.* **2011**, *9*, 552–560. [CrossRef]
4. Gao, G.; Beardall, J.; Jin, P.; Gao, L.; Xie, S.; Gao, K. A Review of Existing and Potential Blue Carbon Contributions to Climate Change Mitigation in the Anthropocene. *J. Appl. Ecol.* **2022**, *59*, 1686–1699. [CrossRef]
5. IPCC. *Climate Change 2013: The Physical Science Basis*; Cambridge University Press: Cambridge, UK, 2013.
6. Krause-Jensen, D.; Duarte, C.M. Substantial Role of Macroalgae in Marine Carbon Sequestration. *Nat. Geosci.* **2016**, *9*, 737–742. [CrossRef]
7. Hurd, C.L.; Law, C.S.; Bach, L.T.; Britton, D.; Hovenden, M.; Paine, E.R.; Raven, J.A.; Tait, L.W.; Boyd, P.W. Forensic Carbon Accounting: Assessing the Role of Seaweeds for Carbon Sequestration. *J. Phycol.* **2022**, *58*, 347–363. [CrossRef] [PubMed]
8. Duarte, C.M.; Gattuso, J.-P.; Hancke, K.; Gundersen, H.; Filbee-Dexter, K.; Pedersen, M.F.; Middelburg, J.J.; Burrows, M.T.; Krumhansl, K.A.; Wernberg, T.; et al. Global Estimates of the Extent and Production of Macroalgal Forests. *Glob. Ecol. Biogeogr.* **2022**, *31*, 1422–1439. [CrossRef]

9. Filbee-Dexter, K.; Wernberg, T. Rise of Turfs: A New Battlefront for Globally Declining Kelp Forests. *BioScience* **2018**, *68*, 64–76. [CrossRef]
10. Filbee-Dexter, K.; Wernberg, T. Substantial Blue Carbon in Overlooked Australian Kelp Forests. *Sci. Rep.* **2020**, *10*, 12341. Correction in *Sci. Rep.* **2020**, *10*, 17253. https://doi.org/10.1038/s41598-020-74313-4. [CrossRef] [PubMed]
11. Gao, G.; Gao, L.; Jiang, M.; Jian, A.; He, L. The Potential of Seaweed Cultivation to Achieve Carbon Neutrality and Mitigate Deoxygenation and Eutrophication. *Environ. Res. Lett.* **2022**, *17*, 014018. [CrossRef]
12. FAO. *The State of World Fisheries and Aquaculture 2024*; FAO: Rome, Italy, 2024.
13. Zhang, J.; Fang, J.; Wang, W.; Du, M.; Gao, Y.; Zhang, M. Growth and Loss of Mariculture Kelp Saccharina japonica in Sungo Bay, China. *J. Appl. Phycol.* **2012**, *24*, 1209–1216. [CrossRef]
14. Gao, K.; McKinley, K.R. Use of Macroalgae for Marine Biomass Production and CO_2 Remediation. *J. Appl. Phycol.* **1994**, *6*, 45–60. [CrossRef]
15. Gao, Y.; Zhang, Y.; Du, M.; Lin, F.; Jiang, W.; Li, W.; Li, F.; Lv, X.; Fang, J.; Jiang, Z. Dissolved Organic Carbon from Cultured Kelp Saccharina japonica: Production, Bioavailability, and Bacterial Degradation Rates. *Aquacult. Environ. Interact.* **2021**, *13*, 101–110. [CrossRef]
16. Kim, J.K.; Yarish, C.; Hwang, E.K.; Park, M.; Kim, Y. Seaweed Aquaculture: Cultivation Technologies, Challenges and Its Ecosystem Services. *Algae* **2017**, *32*, 1–13. [CrossRef]
17. Liang, Z.; Wang, W.; Liu, L.; Li, G.; Xia, B. Influence of Commercial-Scale Seaweed Cultivation on Water Quality: A Case Study in a Typical Laver Culture Area of the Yellow Sea, North China. *J. Mar. Sci. Eng.* **2022**, *10*, 681. [CrossRef]
18. Yang, Y.; Xiong, Y.; Wang, T.; Zhang, J.; Feng, L.; Gao, G. Seaweed and Shellfish Mariculture as Nature-Based Solutions: Mitigating Nutrient Pollution from Coastal Fish Mariculture and Sewage. *Mar. Pollut. Bull.* **2026**, *222*, 118793. [CrossRef] [PubMed]
19. Guo, S.; Nie, H. Estimation of Mariculture Carbon Sinks in China and Its Influencing Factors. *J. Mar. Sci. Eng.* **2024**, *12*, 724. [CrossRef]
20. Quan, W.; Ying, M.; Kang, H. Marine Algae Culture and the Estimation of Carbon Sink Capacity in the Coastal Areas of China. *J. Fish. China* **2014**, *38*, 509–514. (In Chinese)
21. Yue, L.; Zhang, Y.; Zou, Z.; Shi, S.; Zhang, Y.; Zhao, Y.; Qu, M.; Fan, W. Mapping the Optimal Marine Zones for Artificial Upwelling and Assessing Its Macroalgae-Based Carbon Sink Potential in China. *Resour. Conserv. Recycl.* **2025**, *222*, 108468. [CrossRef]
22. Tang, Q.; Zhang, J.; Fang, J. Shellfish and Seaweed Mariculture Increase Atmospheric CO_2 Absorption by Coastal Ecosystems. *Mar. Ecol. Prog. Ser.* **2011**, *424*, 97–104. [CrossRef]
23. Chopin, T. Aquaculture Integrated Multi-Trophic Aquaculture: A Historical Perspective. In *Encyclopedia of Sustainability Science and Technology*; Meyers, R.A., Ed.; Springer: New York, NY, USA, 2012; pp. 184–211.
24. Troell, M.; Joyce, A.; Chopin, T.; Neori, A.; Buschmann, A.H.; Fang, J.-G. Ecological Engineering in Aquaculture: Potential for Integrated Multi-Trophic Aquaculture in Marine Offshore Systems. *Aquaculture* **2009**, *297*, 1–9. [CrossRef]
25. Bindoff, N.L.; Cheung, W.W.L.; Kairo, J.G.; Arístegui, J.; Guinder, V.A.; Hallberg, R.; Hilmi, N.; Jiao, N.; Karim, M.S.; Levin, L.; et al. Changing Ocean, Marine Ecosystems, and Dependent Communities. In *IPCC Special Report on the Ocean and Cryosphere in a Changing Climate*; IPCC: Geneva, Switzerland, 2019.
26. Breiman, L. Random Forests. *Mach. Learn.* **2001**, *45*, 5–32. [CrossRef]
27. Li, C.; Yan, N.; He, Y. China's Marine Carbon Sink Capacity Assessment and Potential Projection: A Machine Learning Approach. *Front. Mar. Sci.* **2026**, *13*, 1839741. [CrossRef]
28. Dong, J.; Liu, Z.; Chen, L. Trading Policy, Practice and Prospect on Marine Carbon Sequestration in China. *Bull. Chin. Acad. Sci.* **2024**, *39*, 519–527. (In Chinese)
29. Fujita, R.; Augyte, S.; Bender, J.; Brittingham, P.; Buschmann, A.H.; Chalfin, M.; Collins, J.; Davis, K.A.; Gallagher, J.B.; Gentry, R.; et al. Seaweed Blue Carbon: Ready? Or Not? *Mar. Policy* **2023**, *155*, 105747. [CrossRef]
30. Ministry of Ecology and Environment of the People's Republic of China; State Administration for Market Regulation. *Measures for the Administration of Voluntary Greenhouse Gas Emission Reduction Trading (Trial) (Order No. 31)*; MEE: Beijing, China, 2023. (In Chinese)
31. Zheng, Y.; Jin, R.; Zhang, X.; Wang, Q.; Wu, J. The Considerable Environmental Benefits of Seaweed Aquaculture in China. *Stoch. Environ. Res. Risk Assess.* **2019**, *33*, 1203–1221. [CrossRef]
32. Ministry of Agriculture and Rural Affairs of the People's Republic of China. *China Fishery Statistical Yearbook 2024*; China Agriculture Press: Beijing, China, 2024. (In Chinese)
33. Kim, J.K.; Yarish, C. Development of a Sustainable Land-Based Gracilaria Cultivation System. *Algae* **2014**, *29*, 217–225. [CrossRef]
34. Li, X.; Wang, K.; Chen, J.; Zhang, S. Allometric Growth of *Sargassum fusiforme* (Ochrophyta, Fucales) Organs in the Maturation Period Based on Biomass Analysis of Samples from Gouqi Island. *J. Mar. Sci. Eng.* **2021**, *9*, 1320. [CrossRef]
35. Sun, J.; Zhao, C.; Zhao, S.; Dai, W.; Liu, J.; Zhang, J.; Xu, J.; He, P. Diversity of CO_2 Concentrating Mechanisms in Macroalgae Photosynthesis: A Case Study of Ulva sp. *J. Mar. Sci. Eng.* **2023**, *11*, 1911. [CrossRef]

36. Wu, H.; Shin, S.K.; Jang, S.; Yarish, C.; Kim, J.K. Growth and Nutrient Bioextraction of *Gracilaria chorda*, *G. vermiculophylla*, *Ulva prolifera*, and *U. compressa* under Hypo- and Hyper-Osmotic Conditions. *Algae* **2018**, *33*, 329–340. [CrossRef]
37. Lü, H.; Ye, G.; Jin, M.; Jia, S. Ecological Service Value Evaluation of Seaweed Aquaculture in Zhejiang and Jiangsu Provinces. *J. Fish. China* **2018**, *42*, 1254–1262. (In Chinese)
38. Cheng, X.; Zhao, X.; Lin, J.; Zhang, S.; Wang, Z.; Huang, H.; Wang, K.; Chen, J. Rotation Culture of Macroalgae Based on Photosynthetic Physiological Characteristics of Algae. *Biology* **2024**, *13*, 459. [CrossRef] [PubMed]
39. Zhai, R.; Tang, C.; Wang, S.; Ma, J.; Li, X.; Chen, G.; Xu, J. Development of a Mitochondrial Marker for Distinguishing Between Uva linza and Ulva prolifera. *J. Mar. Sci. Eng.* **2025**, *13*, 632. [CrossRef]
40. Zhejiang Provincial Department of Ecology and Environment. *Zhejiang Province Marine Environment Bulletin*; Zhejiang Provincial Department of Ecology and Environment: Hangzhou, China, 2023.
41. Hyndman, R.J.; Athanasopoulos, G. *Forecasting: Principles and Practice*, 2nd ed.; OTexts: Melbourne, Australia, 2018.
42. Pessarrodona, A.; Franco-Santos, R.M.; Wright, L.S.; Vanderklift, M.A.; Howard, J.; Pidgeon, E.; Wernberg, T.; Filbee-Dexter, K. Carbon Sequestration and Climate Change Mitigation Using Macroalgae: A State of Knowledge Review. *Biol. Rev.* **2023**, *98*, 1945–1971. [CrossRef] [PubMed]
43. Rose, D.J.; Hemery, L.G. Methods for Measuring Carbon Dioxide Uptake and Permanence: Review and Implications for Macroalgae Aquaculture. *J. Mar. Sci. Eng.* **2023**, *11*, 175. [CrossRef]
44. *HY/T 0305—2021*; Estimation Method of Maricultural Seaweed and Bivalve Carbon Sink—Carbon Stock Variation Method. Ministry of Natural Resources of the People's Republic of China: Beijing, China, 2021. (In Chinese)
45. Liu, C.; Liu, G.; Casazza, M.; Yan, N.; Xu, L.; Hao, Y. Current Status and Potential Assessment of China's Ocean Carbon Sinks. *Environ. Sci. Technol.* **2022**, *56*, 6584–6595. [CrossRef] [PubMed]
46. Watanabe, K.; Yoshida, G.; Hori, M.; Umezawa, Y.; Moki, H.; Kuwae, T. Macroalgal Metabolism and Lateral Carbon Flows Can Create Significant Carbon Sinks. *Biogeosciences* **2020**, *17*, 2425–2440. [CrossRef]
47. Paine, E.R.; Schmid, M.; Boyd, P.W.; Diaz-Pulido, G.; Hurd, C.L. Rate and Fate of Dissolved Organic Carbon Release by Seaweeds: A Missing Link in the Coastal Ocean Carbon Cycle. *J. Phycol.* **2021**, *57*, 1375–1391. [CrossRef] [PubMed]
48. Froehlich, H.E.; Afflerbach, J.C.; Frazier, M.; Halpern, B.S. Blue Growth Potential to Mitigate Climate Change through Seaweed Offsetting. *Curr. Biol.* **2019**, *29*, 3087–3093. [CrossRef] [PubMed]
49. Fourqurean, J.W.; Duarte, C.M.; Kennedy, H.; Marbà, N.; Holmer, M.; Mateo, M.A.; Apostolaki, E.T.; Kendrick, G.A.; Krause-Jensen, D.; McGlathery, K.J.; et al. Seagrass Ecosystems as a Globally Significant Carbon Stock. *Nat. Geosci.* **2012**, *5*, 505–509. [CrossRef]
50. Ouyang, X.; Lee, S.Y. Updated Estimates of Carbon Accumulation Rates in Coastal Marsh Sediments. *Biogeosciences* **2014**, *11*, 5057–5071. [CrossRef]
51. Krause-Jensen, D.; Lavery, P.; Serrano, O.; Marbà, N.; Masque, P.; Duarte, C.M. Sequestration of Macroalgal Carbon: The Elephant in the Blue Carbon Room. *Biol. Lett.* **2018**, *14*, 20180236. [CrossRef] [PubMed]
52. Duarte, C.M.; Agusti, S.; Barbier, E.; Britten, G.L.; Castilla, J.C.; Gattuso, J.-P.; Fulweiler, R.W.; Hughes, T.P.; Knowlton, N.; Lovelock, C.E.; et al. Rebuilding Marine Life. *Nature* **2020**, *580*, 39–51. Correction in *Nature* **2021**, *593*, E1–E2. https://doi.org/10.1038/s41586-021-03271-2. [CrossRef] [PubMed]
53. Mendoza-Segura, C.; Fernández, E.; Beca-Carretero, P. Predicted Changes in the Biogeographical Range of Gracilaria vermiculophylla under Present and Future Climate Scenarios. *J. Mar. Sci. Eng.* **2023**, *11*, 367. [CrossRef]
54. Jiao, N.; Herndl, G.J.; Hansell, D.A.; Benner, R.; Kattner, G.; Wilhelm, S.W.; Kirchman, D.L.; Weinbauer, M.G.; Luo, T.; Chen, F.; et al. Microbial Production of Recalcitrant Dissolved Organic Matter: Long-Term Carbon Storage in the Global Ocean. *Nat. Rev. Microbiol.* **2010**, *8*, 593–599. [CrossRef] [PubMed]

Disclaimer/Publisher's Note: The statements, opinions and data contained in all publications are solely those of the individual author(s) and contributor(s) and not of MDPI and/or the editor(s). MDPI and/or the editor(s) disclaim responsibility for any injury to people or property resulting from any ideas, methods, instructions or products referred to in the content.